



ACVR1/ALK2-p21 signaling axis modulates proliferation of the venous endothelium in the retinal vasculature

Boryeong Pak¹ · Minjung Kim¹ · Orjin Han¹ · Heon-Woo Lee^{2,6} · Alexandre Dubrac^{2,3} · Woosung Choi¹ · Jee Myung Yang⁴ · Kevin Boyé² · Heewon Cho¹ · Kathryn M. Citrin⁵ · Injune Kim⁴ · Anne Eichmann² · Victoria L. Bautch⁵ · Suk-Won Jin^{1,2}

Received: 4 March 2024 / Accepted: 18 June 2024
© The Author(s), under exclusive licence to Springer Nature B.V. 2024

Abstract

The proliferation of the endothelium is a highly coordinated process to ensure the emergence, expansion, and homeostasis of the vasculature. While Bone Morphogenetic Protein (BMP) signaling fine-tunes the behaviors of endothelium in health and disease, how BMP signaling influences the proliferation of endothelium and therefore, modulates angiogenesis remains largely unknown. Here, we evaluated the role of Activin A Type I Receptor (ACVR1/ALK2), a key BMP receptor in the endothelium, in modulating the proliferation of endothelial cells. We show that ACVR1/ALK2 is a key modulator for the proliferation of endothelium in the retinal vessels. Loss of endothelial ALK2 leads to a significant reduction in endothelial proliferation and results in fewer branches/endothelial cells in the retinal vessels. Interestingly, venous endothelium appears to be more susceptible to ALK2 deletion. Mechanistically, ACVR1/ALK2 inhibits the expression of CDKN1A/p21, a critical negative regulator of cell cycle progression, in a SMAD1/5-dependent manner, thereby enabling the venous endothelium to undergo active proliferation by suppressing CDKN1A/p21. Taken together, our findings show that BMP signaling mediated by ACVR1/ALK2 provides a critical yet previously underappreciated input to modulate the proliferation of venous endothelium, thereby fine-tuning the context of angiogenesis in health and disease.

Keywords BMP signaling · ALK2/ACVR1 · p21/CDKN1A · Endothelium · Cell cycle

Boryeong Pak, Minjung Kim, Orjin Han and Heon-Woo Lee have equally contributed.

✉ Suk-Won Jin
sukwonjin@gist.ac.kr

¹ School of Life Sciences and Cell Logistics Research Center, Gwangju Institute of Science and Technology (GIST), Gwangju, Korea

² Yale Cardiovascular Research Center, Section of Cardiovascular Medicine, Department of Internal Medicine, Yale University School of Medicine, New Haven, CT, USA

³ CHU Sainte-Justine Research Center, and Department of Pathology and Cellular Biology, Université de Montréal, Montréal, QC, Canada

⁴ Graduate School of Medical Science and Engineering, Korea Advanced Institute of Science and Technology (KAIST), Daejeon, Korea

⁵ Department of Biology and McAllister Heart Institute, University of North Carolina, Chapel Hill, NC, USA

⁶ Present Address: Department of Pharmacy, Chosun University, Gwangju, Korea

Introduction

The formation of new blood vessels entails an adequate and continuous supply of endothelial cells (ECs) from pre-existing vessels to angiogenic sites. This process requires the generation of new ECs serving as building blocks for forming new vessels. Accordingly, well-characterized ‘pro-angiogenic’ cues are known to stimulate and induce robust proliferation of ECs [1]. Therefore, to effectively manipulate angiogenesis with physiological relevance, it is imperative to comprehend the intricate mechanisms governing the regulation of EC proliferation. Recent advances using mouse models have identified the pivotal role of Notch and Vascular Endothelial Growth Factor (VEGF) signaling pathways in regulating the proliferative capacity of ECs in vivo [2]. However, the relationship between the activity of these signaling pathways and EC proliferation is complex.

For instance, Notch signaling, which is induced by blood flow [3], induces the expression of CDKN1B/p27, a negative regulator of cell cycle progression, in a Connexin 37 (GJA4/

Cx37)-dependent manner, thereby limiting the proliferation of ECs exposed to high blood flow [4]. However, Notch-mediated regulation of EC proliferation is biphasic, as lack of Notch signaling also blocks cell cycle progression and attenuates EC proliferation [2]. Similarly, VEGF signaling also modulates EC proliferation in a biphasic manner, as excessive ERK1/2 activation induced by VEGF signaling, which is generally considered a pro-angiogenic cue, elevates CDKN1A/p21 expression, causing mitotic arrest in ECs [5]. While somewhat paradoxical to the prevailing idea obtained from in vitro cell culture studies, these recent studies provide substantial progress toward a better understanding of how EC proliferation is regulated in vivo. To fully grasp the complexity of the molecular mechanisms whereby cell cycle progression and subsequent EC proliferation are coordinated, it is essential to analyze how additional signaling pathways implicated in modulating EC behavior contribute to this intricate process.

Bone Morphogenetic Protein (BMP) signaling is one of the archetypal signaling pathways that governs various cellular behaviors, including migration, differentiation, and proliferation [6]. In ECs, BMP signaling induces both endothelial sprouting during angiogenesis and maintains vascular homeostasis in culture and in vivo [7, 8]. Dysregulation of BMP signaling leads to diverse human diseases and pathological conditions linked to vascular diseases, including pulmonary arterial hypertension, hereditary hemorrhagic telangiectasia, and cerebral cavernous malformation, as mutations in the key components of BMP signaling have been implicated in the onset of these diseases [9–11]. To date, an array of Type 1 receptors, including Activin A Type 1 Receptor-Like (ALK1/ACVRL1) [12], Activin A Type I Receptor (ALK2/ACVR1) [13], and Bone Morphogenetic Protein Type 1 Receptor (ALK3/BMPR1A) [14], are known to be expressed in ECs. While ALK2 and ALK3 have been implicated in transducing pro-angiogenic/anti-lymphangiogenic BMP signaling [13], ALK1 mediates anti-angiogenic/pro-lymphangiogenic BMP signaling, which sets it apart from the rest of the BMPR1s [15].

BMP signaling appears to elicit distinct signaling outcomes in endothelial cells in a context-dependent manner [16–18]. For instance, previous studies have shown that inputs from the BMP signaling are more critical for venous ECs; BMP signaling induces angiogenic responses preferentially from venous ECs in zebrafish [14, 19–21], and BMPR1A/ALK3 is implicated to be essential for the specification of venous ECs in both mice and zebrafish [14]. Moreover, arterial ECs appear relatively unresponsive to BMP signaling, except for the ACVRL1/ALK1-mediated anti-angiogenic BMP9/10 signaling [15, 22–24]. While BMP signaling has been shown to modulate cell proliferation in various cell types [20, 24–26] and has been

implicated in endothelial proliferation, detailed molecular mechanisms whereby BMP signaling modulates endothelial proliferation have not been fully elucidated. In this report, we aim to examine this possibility and present evidence that ACVR1/ALK2-mediated BMP signaling is essential to promote endothelial proliferation in the retinal vasculature. Interestingly, we find that venous endothelial cells appear to be more sensitive to the lack of endothelial ACVR1/ALK2. Considering that venous ECs predominantly contribute to most newly formed ECs during angiogenesis [27], our findings suggest that BMP signaling conferred by ACVR1/ALK2 is critical in determining the angiogenic potential of the vasculature in both health and disease.

Materials and methods

Detailed materials and methods can be found in the supplementary materials. All data, analytic methods, and study materials supporting the findings of this study are provided in the article and supplemental material and are available from the corresponding author upon reasonable request.

Animals

The experiments were conducted according to NIH guidelines on the use of laboratory animals, and the research protocols were approved by the Yale University IACUC and Gwangju Institute of Science and Technology IACUC. The *Alk2^{fllox/fllox}*, and *Cdh5(PAC)-CreER^{T2}* mice were previously described [28, 29]. To acquire *Alk2* endothelial-specific deleted retinas, P1 to P3 pups were intraperitoneally administered with 50 µg tamoxifen in corn oil (Sigma, T5648; 10 mg/mL dissolved in corn oil). 1 mg tamoxifen was sequentially administered into E6.5 to E7.5 embryo-bearing female mice by intraperitoneal injection. Subsequently, the pregnant female mice were sacrificed at designated stages. All mice were euthanized using the carbon dioxide (CO₂) incubation protocol except those used for fresh EC isolation. For EC isolation, the cervical dislocation method was used to prevent any changes to the molecular properties of ECs that could result from CO₂ overdose.

Mouse retina preparation

Neonatal mouse eyes at chosen stages were collected after 8-min CO₂ euthanization and then fixed in 4% paraformaldehyde (PFA), and the cornea, eyeball, and the most-outer layer were removed. The dissected retinas were incubated in permeabilization buffer (1% FBS, 3% BSA, 0.5% Triton X-100, 0.01% Na-deoxycholate, and 0.02% Na-azide in PBS or TBS). For the following purposes, the

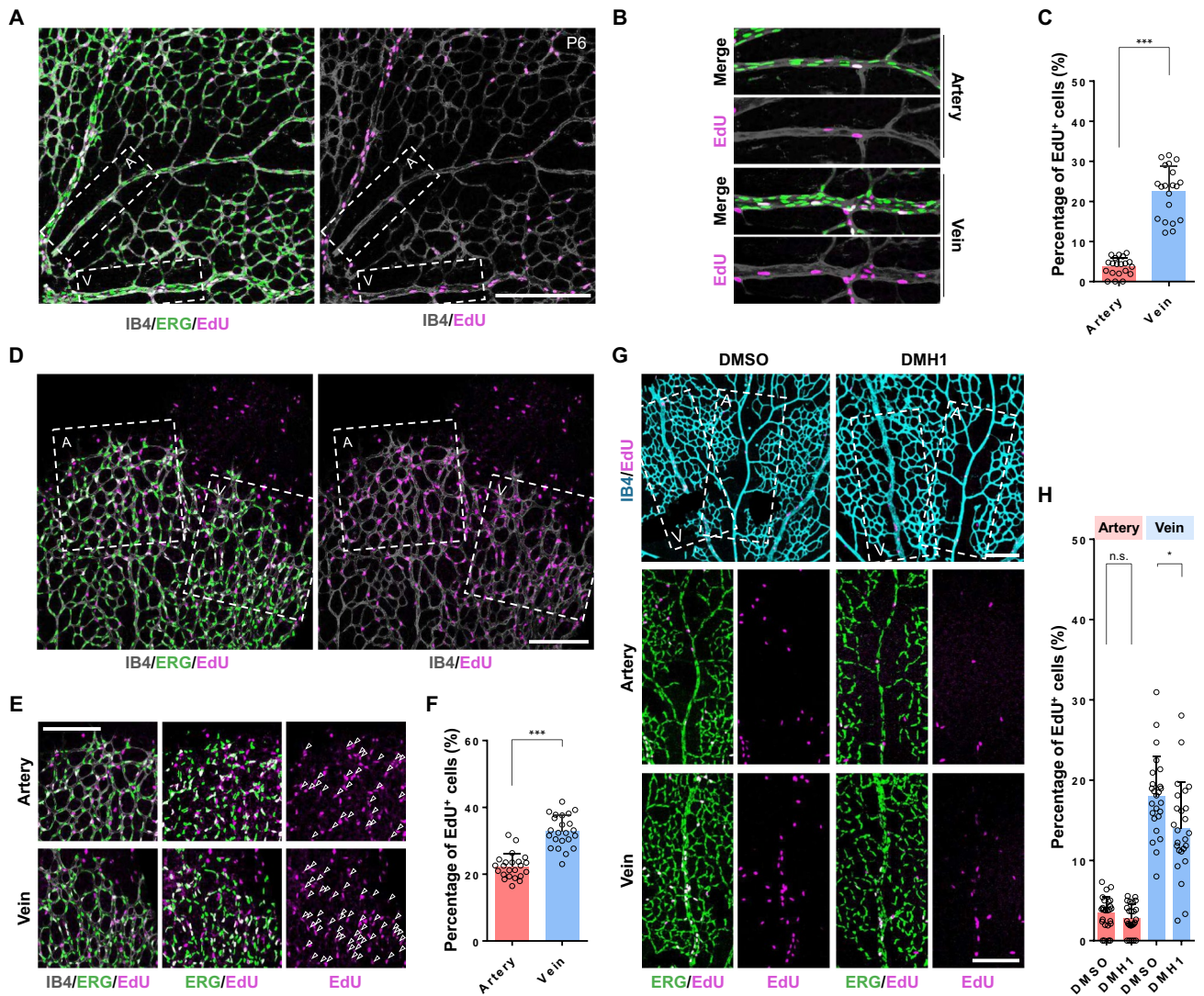


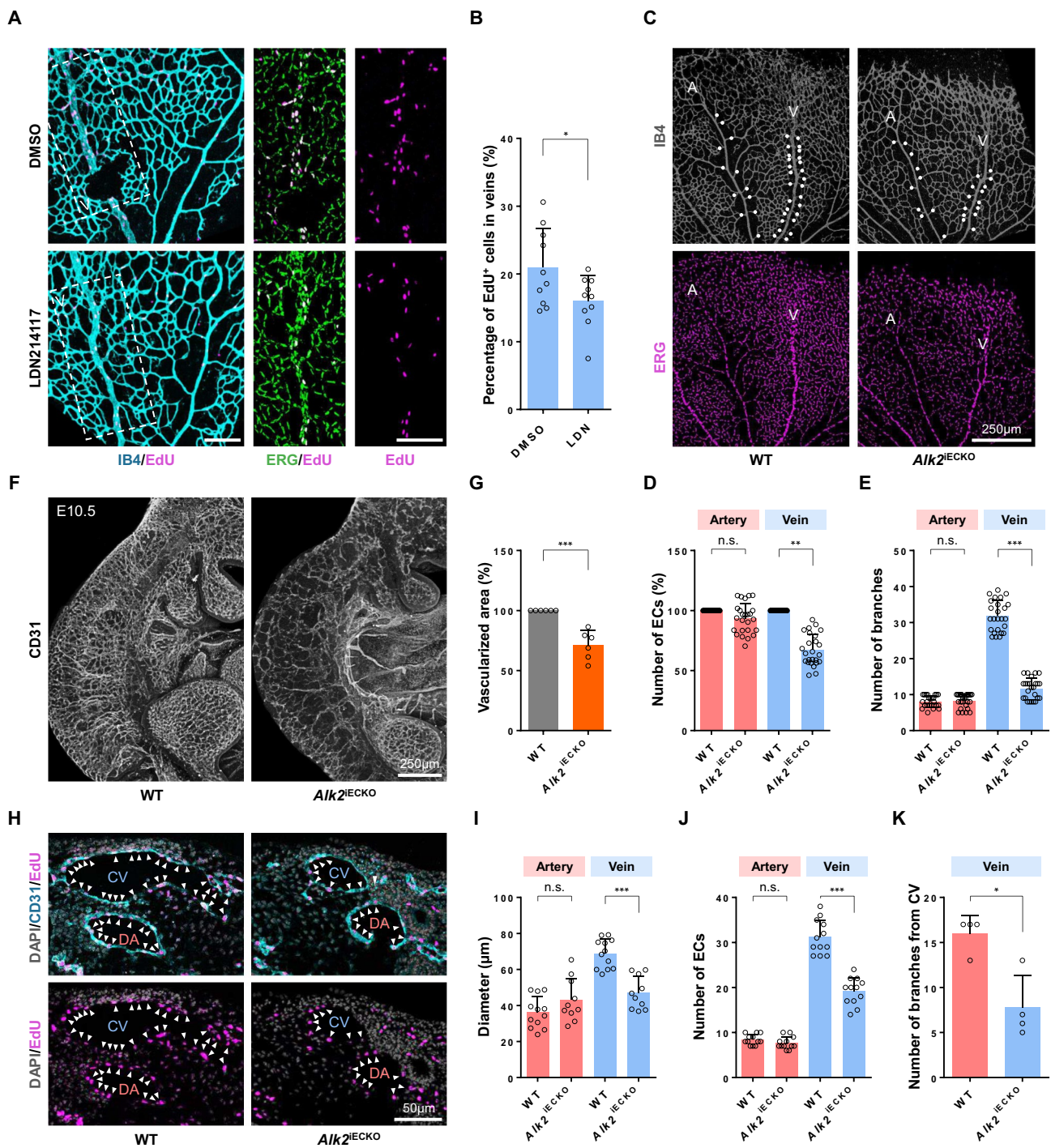
Fig. 1 BMP signaling promotes proliferation of venous endothelium in the retina. **A** Venous ECs are more proliferative than arterial ECs in the retinal vasculature. (Colors: IB4 (grey), ERG1/2/3 (green), and EdU (magenta); Symbols: A = artery, V = vein; Scale bar = 200 μ M). **B** The areas within white dotted rectangles in panel A are shown at a higher magnification. (Colors: IB4 (grey), ERG1/2/3 (green), and EdU (magenta); Scale bar = 100 μ M). **C** Percentage of proliferating ECs ($\text{EdU}^+/\text{ERG}^+$) relative to total ECs (ERG^+) in arteries or veins shown in panel A. ($n=3$ (40 vessels from 5 retinas), $***P < 0.0005$ (unpaired t -test)). **D** Front area of P6 retina. (Colors: IB4 (grey), ERG (ERG1/2/3, green), and EdU (magenta); Symbols: A = artery, V = vein; Scale bar = 100 μ M). **E** The white dashed rectangles in panel D are shown at a higher magnification. White empty arrowheads indicate EdU^+ EC in the artery-stemmed (Artery) and vein-

stemmed area (Vein). (Colors: IB4 (grey), ERG (ERG1/2/3, green), and EdU (magenta); Scale bar = 50 μ M). **F** Percentage of proliferating ECs ($\text{EdU}^+/\text{ERG}^+$) relative to total ECs (ERG^+) in arterial or venous regions shown in panel D. ($n=3$ (50 vessels from 7 retinas), $***P < 0.0005$ (unpaired t -test)). **G** Chemical inhibition of BMP signaling decreases proliferation in venous ECs. DMSO (left) or DMH1 (right) was intraperitoneally injected. (Colors: IB4 (cyan), ERG1/2/3 (green), and EdU (magenta); Symbols: A = artery, V = vein; Scale bar = 200 μ M). **H** Percentage of proliferating ECs ($\text{EdU}^+/\text{ERG}^+$) relative to total ECs (ERG^+) in arteries (red) or veins (blue) shown in panel G. ($n=3$ (50 vessels from 6 retinas), n.s. = not significant, $*P < 0.05$ (one-way ANOVA with post hoc unpaired t -test))

retinas were washed with PBS three times and incubated in staining solution with primary antibodies.

Oxygen-induced retinopathy model

To generate oxygen-induced retinopathy (OIR) mice, nursing females, and P7 neonatal pups were exposed to 75% O_2 (hyperoxia) for five days. Then, the P12-old pups were placed in room air (normoxia). The induced pups were



sacrificed, and their retinas were harvested at desired time points (P14 and P17). *Alk2* endothelial-specific deleted retinas of the OIR model were acquired by tamoxifen-induced Cre recombinase activation at P11 and P12. 200 μg of tamoxifen was administrated by intraperitoneal (IP) injection. Subsequently, the pups were sacrificed, and their eyes were collected in 4% PFA. Retinas dissected using microsurgical scissors and tweezers were stained and flat-mounted on

a glass slide. Images were captured using Leica SP5 confocal microscope.

Quantification and statistical analyses

Signal intensity of fluorescent images and immunoblot were quantified using ImageJ. The number of ECs in retinal arteries and veins was quantified manually. We defined

Fig. 2 ALK2 is required for endothelial proliferation in vivo. **A** Treatment of LDN214117 decreases proliferation in venous ECs by inhibiting ALK2 activity. DMSO or LDN214117 was intraperitoneally injected as a control or test treatment, respectively. The white dashed rectangles are shown at a higher magnification in the right panels. (Colors: IB4 (cyan), ERG1/2/3 (green), and EdU (magenta); Symbols: V=vein; Scale bar=100 μ M). **B** Percentage of proliferating ECs (EdU⁺/ERG⁺) relative to total ECs (ERG⁺) in veins shown in panel A. ($n=3$ (20 veins from 6 retinas), $*P<0.05$ (unpaired t -test)). **C** P6 retinal vasculature of littermates (left panels) and $Alk2^{\text{IECKO}}$ (right panels). (Colors: IB4 (grey) and ERG1/2/3 (magenta); Symbols: A=artery, V=vein; Scale bar=250 μ M). White dots point to branch points within arteries and veins. **D–E** Quantification of the number of ECs (**D**; $n=3$ (50 vessels from 8 retinas), n.s.=not significant, $**P<0.005$ (one-way ANOVA with post hoc unpaired t -test)) and the number of branches from the artery and vein (**E**; $n=3$ (50 vessels from 8 retinas), n.s.=not significant, $***P<0.0005$ (one-way ANOVA with post hoc unpaired t -test)) from the images shown in panel C. **F** CD31 immunostaining of E10.5 WT or $Alk2^{\text{IECKO}}$ embryos. (Scale bar=250 μ M). **G** Quantification of the vascularized area within embryos shown in panel F. ($n=2$ (6 WT and 6 $Alk2^{\text{IECKO}}$ embryos), $***P<0.0005$ (unpaired t -test)). **H** Representative transverse sections of E10.5 WT or $Alk2^{\text{IECKO}}$ embryos. The cardinal vein is more affected by endothelial deletion of $Alk2$. (Colors: CD31 (cyan), ERG1/2/3 (magenta), and DAPI (white); Symbols: DA=dorsal aorta, CV=cardinal vein; Scale bar=50 μ M). White arrowheads point to CD31 and ERG1/2/3 double-positive endothelial nuclei. **I–J** Quantification of the diameter (**I**; $n=3$ (12 WT and 10 $Alk2^{\text{IECKO}}$ embryos), n.s.=not significant, $***P<0.0005$ (one-way ANOVA with post hoc unpaired t -test)) and the number of ECs (**J**; $n=3$ (12 WT and 10 $Alk2^{\text{IECKO}}$ embryos), n.s.=not significant, $***P<0.0005$ (one-way ANOVA with post hoc unpaired t -test)) of the dorsal aorta (DA, red) and cardinal vein (CV, blue) shown in panel H. **K** Quantification of the number of branch points from the cardinal vein. ($n=2$ (4 WT and 4 $Alk2^{\text{IECKO}}$ embryos), $*P<0.05$ (unpaired t -test))

arteries and veins as the main vessels extending from the optic disc to the peripheral regions where vessels branch out. All statistical analyses were performed using GraphPad Prism software. For comparisons between two groups, we employed the unpaired Student's t -test with Welch's correction to calculate p -values. For comparisons with more than two groups, we used a one-way ANOVA followed by post-hoc unpaired Student's t -tests. n represents the number of biological replicates used in the statistical analysis. Each replicate comprised a control sample and a corresponding test sample treated with either reagent, siRNA, or $Alk2^{\text{IECKO}}$. p -value (n.s.=no significant change, $*p<0.05$, $**p<0.005$, $***p<0.0005$).

Results

BMP signaling modulates proliferation of the endothelium in the retina

To investigate how endothelial proliferation is coordinated between arterial and venous ECs during vascular expansion,

we first examined the murine retinal vasculature. At postnatal day 6 (P6), veins contained six times more EdU-positive (EdU⁺) ECs than arteries, suggesting that venous ECs are more proliferative than arterial ECs (Fig. 1A–C). However, at the vascular front, where new capillaries sprout from the main arteries and veins, the difference in the number of EdU⁺ cells between arterial and venous regions becomes less pronounced compared to the area closer to the optic disc (Fig. 1D–F). This observation is consistent with previous reports showing that sustained proliferation of venous ECs is essential for retinal angiogenesis and arteriogenesis, as the difference in endothelial proliferation between arteries and veins seems to be diminished near the vascular front [30, 31]. Importantly, the striking disparity in the proliferative capacity between arterial and venous ECs was not limited to the retinal and postnatal vasculature, as venous ECs at embryonic day 9.5 (E9.5) similarly showed more EdU⁺ ECs in veins than in arteries (Suppl. Fig. 1A, B). Based on our findings, we postulated that there was a factor that preferentially promotes the proliferation of venous ECs. Since BMP signaling functions as a selective angiogenic cue for venous ECs in zebrafish [20], we sought to ascertain whether BMP signaling similarly serves as a selective proliferative cue for venous ECs in the murine retinal vasculature. Intraperitoneal injection of DMH1, which inhibited BMP signaling (Suppl. Fig. 1C), substantially decreased the number of EdU⁺ venous ECs in retinal vessels (Fig. 1G, H), suggesting that BMP signaling is necessary to support the sustained proliferation of venous ECs in the retinal vasculature.

ALK2 enables BMP-induced proliferation in endothelium

As BMP signaling within the cell needs to be initiated by the surface receptors in a cell-autonomous manner, we wished to identify a key receptor that mediates the BMP-induced endothelial proliferation in the retina. We first assessed the protein distribution of each BMP receptor in the retinal vasculature (Suppl. Fig. 2A) and found that ALK2 protein was enriched in venous ECs as previously reported [13], while ALK1 protein broadly expressed. Based on this finding, we hypothesized that ACVR1/ALK2 may function as a primary receptor that relays BMP-induced venous endothelial proliferation. Corroborating this idea, treatment with LDN214117, a specific ALK2 inhibitor [32, 33], significantly decreased the proliferation of venous ECs in murine retinal vasculature (Fig. 2A, B, and Suppl. Fig. 2B, C).

To further examine the role of ALK2 in relaying BMP stimulation in endothelial cells within the retinal vasculature, we examined vascular defects in mice with inducible endothelial-specific deletion of $Alk2$ ($Alk2^{\text{IECKO}}$ hereafter) and evaluated the phenotype of $Alk2^{\text{IECKO}}$ mice (Suppl. Fig. 3A). We found that the number of ECs and branches

in the veins were significantly reduced in *Alk2*^{iECKO} mice compared to WT mice (Fig. 2C–E), while those from the artery were largely unaffected. Therefore, our data suggest that the morphological defects caused by *Alk2* deletion stem from a selective decrease in the number of ECs within the venous vascular beds.

Consistent with the defects in the retinal vasculature, endothelial deletion of *Alk2* at embryonic stages at E6.5–7.5, CD31-positive blood vessels were significantly reduced in the embryos, resulting in the formation of avascular regions throughout the E10.5 embryos (Fig. 2F, G) without affecting the overall gross morphology of embryos (Suppl. Fig. 3B). Of note, the morphology of veins was more severely affected compared to the arteries in E10.5 *Alk2*^{iECKO} embryos. The diameter and number of ECs in the cardinal vein were significantly reduced in *Alk2*^{iECKO} embryos compared to wild-type littermates, while those of the dorsal aorta remain largely unaltered (Fig. 2H–J). In addition, the secondary angiogenic vessels from the cardinal vein were significantly reduced upon *Alk2* deletion (Fig. 2K). Moreover, pSMAD1/5 deposition appears to be decreased in the veins of the retinal vasculature in *Alk2*^{iECKO} pups (Suppl. Fig. 3C, D). Taken together, our data suggest that ALK2 is a key receptor that mediates BMP signaling to modulate proliferation in venous ECs.

ALK2 is essential for endothelial proliferation in vivo

As angiogenic expansion in the veins was decreased in *Alk2*^{iECKO} mice, we postulated that ALK2 is essential to either sustain the proliferation of venous ECs or to promote the survival of venous ECs. To distinguish these two possibilities, we first examined the effects of ALK2 inhibition on EC survival. In HUVECs, attenuation of *ALK2* by siRNA depletion did not increase the number of caspase-3-positive apoptotic cells (Suppl. Fig. 4A–G). Consistent with this observation, ECs in the retinal vasculature of P7 *Alk2*^{iECKO} pups nor the lung ECs isolated from *Alk2*^{iECKO} mouse-activated caspase-3-dependent cell death (Suppl. Fig. 4H–J). Therefore, it is conceivable that the pronounced vascular defects in *Alk2*^{iECKO} mice were not caused by excessive cell death in ECs. Conversely, HUVECs treated with *ALK2* siRNA showed a significant decrease in both the total number of ECs and the number of EdU⁺ ECs compared to control siRNA-treated HUVECs (Fig. 3A–C). Furthermore, the number of phospho-Histone3-positive ECs was similarly decreased in *ALK2* siRNA-treated HUVECs (Fig. 3D, E). Taken together, our data suggest that lack of *ALK2* is detrimental to EC proliferation but not survival.

In murine embryos, deletion of *Alk2* in ECs led to similar effects on endothelial proliferation. Compared to wild-type littermates, E9.5 *Alk2*^{iECKO} embryos displayed a

reduced number of ECs within the cardinal vein, while the number within the dorsal aorta was unaltered (Fig. 3F, G). Concomitantly, the number of EdU⁺ ECs in the cardinal vein, but not in the dorsal aorta, was decreased in *Alk2*^{iECKO} mice (Fig. 3H). This result suggests that the reduced proliferation of venous ECs is responsible for the decreased number of EC in the cardinal vein of *Alk2*^{iECKO} mice. Similarly, postnatal retinal vasculature (P6) of *Alk2*^{iECKO} mice displayed a reduced number of EC as well as EdU⁺ ECs in the venous plexus (Fig. 3I–K), suggesting that venous ECs remain more susceptible to the lack of ALK2 than arterial ECs during postnatal angiogenesis. The impact of endothelial ALK2 deletion does not stem from morphological changes in adjacent tissues, as the astrocyte scaffold appears to remain unaltered in *Alk2*^{iECKO} mice (Suppl. Fig. 5A, B). Interestingly, ECs near the vascular front display a lower susceptibility to endothelial *Alk2* deletion (Suppl. Fig. 5C, D), reiterating the idea that additional factors influence the proliferation of ECs within or in the vicinity of the vascular front.

To further assess the effects of *Alk2* deletion on endothelial proliferation and cell cycle progression, we examined the relative proportion of *ALK2* siRNA-treated HUVECs across G1, G2/M, and S phases using flow cytometry (Suppl. Fig. 6A, B). Compared to control siRNA treated HUVECs, *ALK2* siRNA treatment resulted in a significant increase in the proportion of cells in S and G2/M phases, which was apparently due to a reduced growth rate. Given the S phase accumulation, potentially reflecting cell cycle arrest, we next explored which specific stage within S phase was affected due to *ALK2* deficiency (Suppl. Fig. 6C). EdU staining revealed that longer EdU treatment resulted in a minimal increase in the early S-phase cell proportion in *ALK2* siRNA-treated HUVECs compared to controls (Suppl. Fig. 6D–F), which suggested that *ALK2* deletion in endothelial cells led to early S phase arrest. Taken together, our data indicate that *Alk2* is a key modulator for cell cycle progression in ECs.

ALK2 promotes pathological angiogenesis in the oxygen-induced retinopathy model

Given that ALK2 promotes proliferation and sprouting angiogenesis of venous ECs developmentally, we asked whether ALK2 exerts a similar function during pathological angiogenesis. We utilized murine oxygen-induced retinopathy (OIR), a widely used experimental model for disease-related angiogenesis [34]. Pups with nursing mothers were exposed to hyperoxic condition (75% oxygen) from P7 to P12 (Fig. 4A) and subsequently returned to room air at P12 to induce excessive proliferation and sprouting angiogenesis within the vaso-obliteration zone (Fig. 4B). Interestingly, in

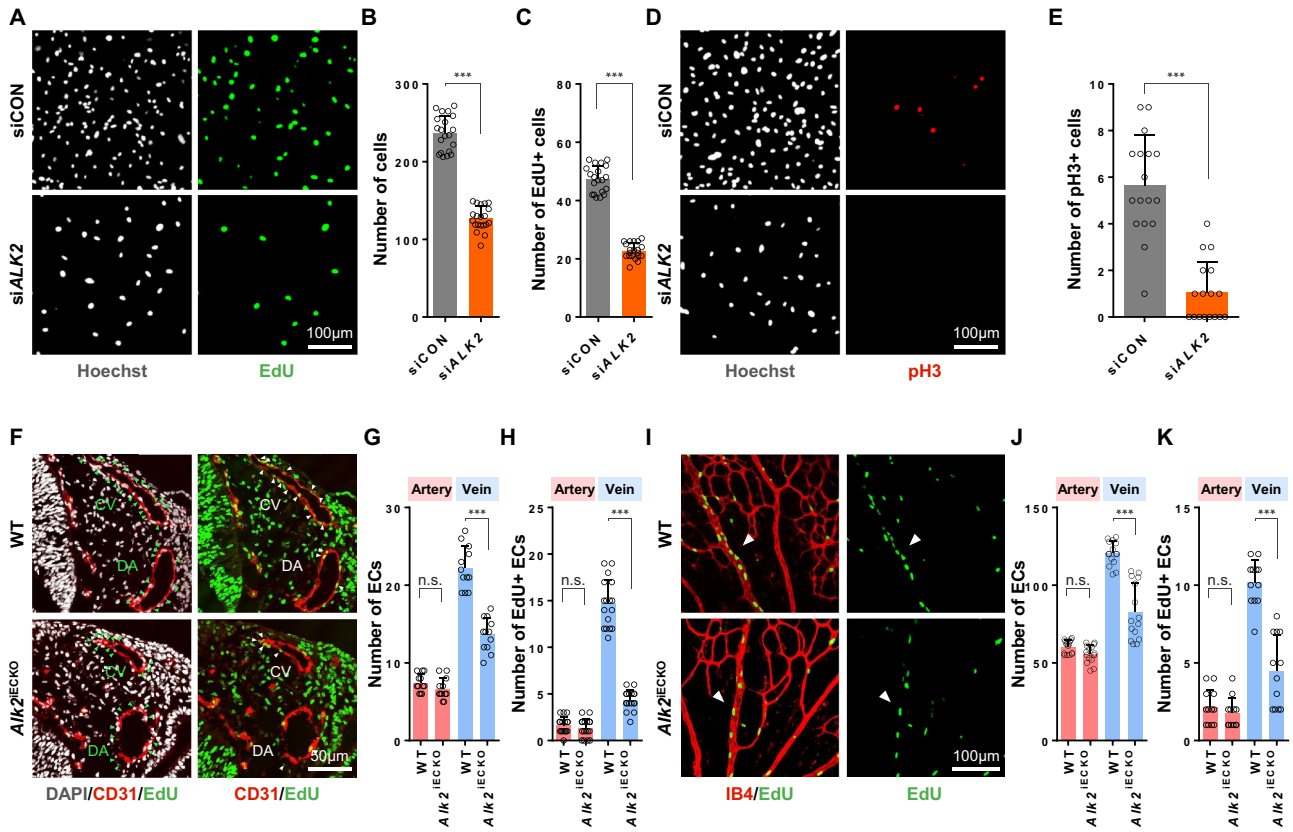


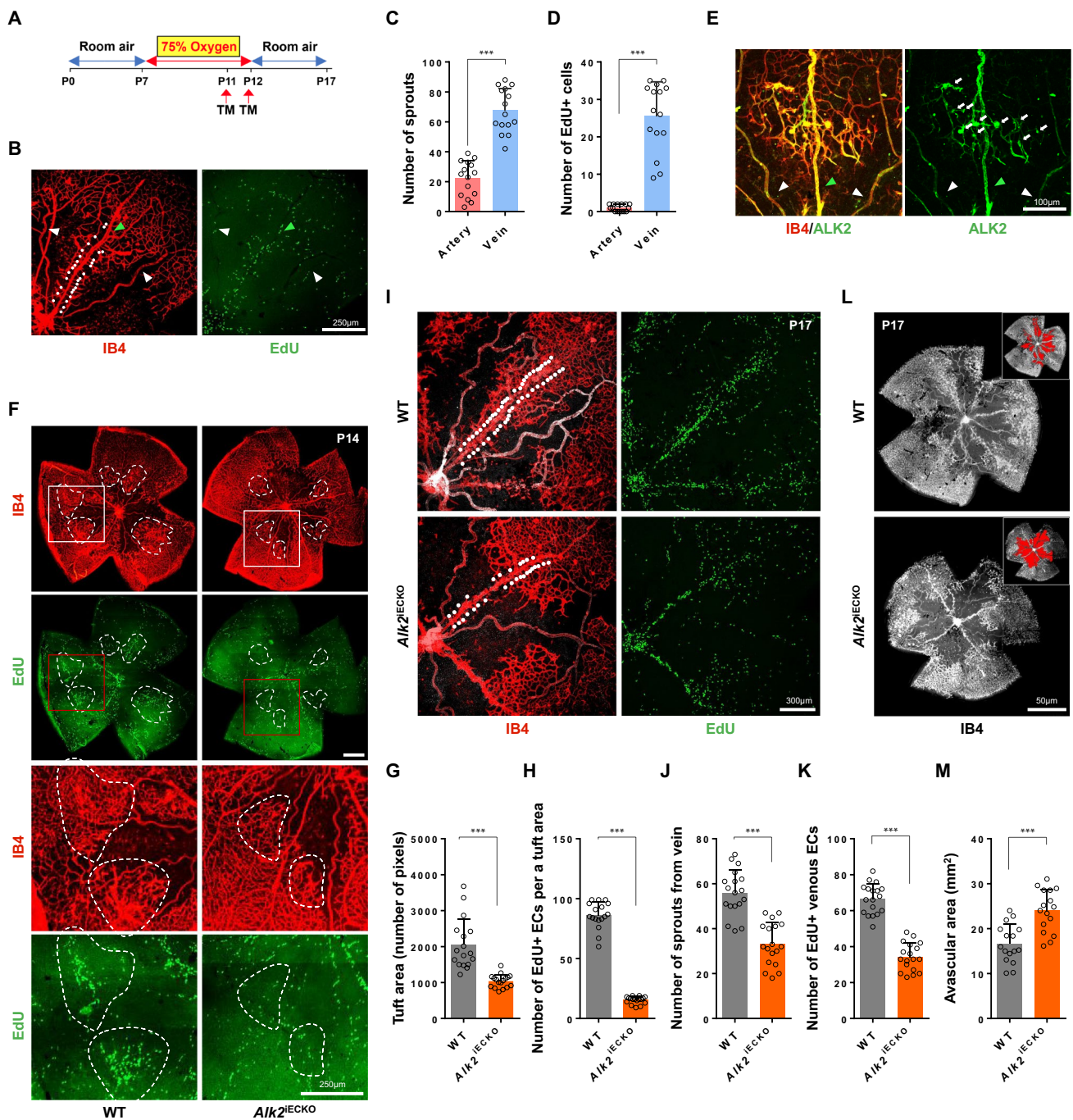
Fig. 3 Lack of ALK2 inhibits proliferation of the venous endothelium. **A** Representative images of HUVECs treated with control or *ALK2* siRNA. (Colors: EdU (green) and Hoechst (white); Scale bar=100 μM). **B–C** Quantification of the total number of cells (**B**; $n=3$ (40 images), $***P<0.0005$ (unpaired *t*-test)) and EdU+ cells (**C**; $n=3$ (40 images), $***P<0.0005$ (unpaired *t*-test)) from panel A. **D** Representative images of pH3 deposition in HUVECs treated with control or *ALK2* siRNA. (Colors: pH3 (red) and Hoechst (white); Scale bar=100 μM). **E** Quantification of pH3-positive cells ($n=3$ (34 images), $***P<0.0005$ (unpaired *t*-test)) from panel D. **F** Images of transverse section of E9.5 wild-type littermates (top panels) and *Alk2*^{iECKO} mice (bottom panels). Green and white arrowheads indicate ECs and EdU+ ECs, respectively. (Colors: CD31 (red), EdU (green), and DAPI (white)); Symbols: DA=dorsal aorta, CV=cardinal vein; Scale bar=50 μM). **G–H** Quantification of the number of

ECs (**G**; $n=4$ (12 WT and 12 *Alk2*^{iECKO} embryos), n.s.=not significant, $***P<0.0005$ (one-way ANOVA with post hoc unpaired *t*-test)) and the number of EdU+ ECs (**H**; $n=4$ (17 WT and 17 *Alk2*^{iECKO} embryos), n.s.=not significant, $***P<0.0005$ (one-way ANOVA with post hoc unpaired *t*-test)) in the cardinal vein (CV, blue) and dorsal aorta (DA, red) shown in panel F. **I** Confocal images of P6 retinal vasculature from WT (top panels) or *Alk2*^{iECKO} mice (bottom panels). White arrowheads point veins. (Colors: IB4 (red), ERG1/2/3 (green), and EdU (magenta); Scale bar=100 μM). **J–K** Quantification of EC number (**J**; $n=3$ (30 vessels from 6 retinas) 11 from three biological replicates, n.s.=not significant, $***P<0.0005$ (one-way ANOVA with post hoc unpaired *t*-test)) and the number of EdU+ ECs (**K**; $n=3$ (24 vessels from 6 retinas), n.s.=not significant, $***P<0.0005$ (one-way ANOVA with post hoc unpaired *t*-test)) in the artery (red) and vein (blue) shown in panel I

the OIR model, sprouting angiogenesis and EdU+ ECs at P14 were predominantly observed in the vein (Fig. 4B–D), suggesting that proliferating venous ECs contribute to the formation of pathological vascular sprouts. Additionally, ALK2 expression was elevated in venous ECs and vascular tufts (Fig. 4E), suggesting that ALK2 contributes to excessive EC proliferation and sprouting angiogenesis in the OIR model.

To further test this possibility, we examined how endothelial deletion of ALK2 affects neovascularization in the OIR model. In vascular tuft areas, where ECs actively undergo proliferation at P14 [34], endothelial-specific

deletion of ALK2 resulted in a substantial reduction of the area with vascular tufts and the number of EdU+ EC compared to those in wild-type littermates (Fig. 4F–H). Moreover, compared to the wild-type littermates, OIR-induced angiogenic sprouts in the vein were significantly reduced in *Alk2*^{iECKO} pups. This reduction was particularly evident in the percentage of EdU+ EC within the venous vascular beds, as demonstrated in the retinas of *Alk2*^{iECKO} pups (Fig. 4H). These defects in the OIR model of *Alk2*^{iECKO} mice consequently led to an increased avascular area at P17 compared to control mice (Fig. 4L, M). Collectively, these findings identify venous ECs as the primary source of ECs



in OIR-induced sprouting angiogenesis and indicate that ALK2 modulates the proliferation of venous ECs, thereby regulating angiogenesis from venous vascular beds in pathological settings.

ALK2 modulates the expression of CDKN1A/p21 to sustain endothelial proliferation

To elucidate the molecular mechanisms through which ALK2 modulates EC proliferation, we next analyzed the

mRNA expression profile of control or ALK2 siRNA-treated HUVECs by RNA-seq (Suppl. Fig. 7A). Gene Ontology (GO) enrichment analysis of genes upregulated by ALK2 knockdown showed that a substantial number of genes were involved in cell cycle-related categories, including the regulation of G0 to G1 transition (Suppl. Fig. 7B, C). To gain deeper mechanistic insight into how ALK2 regulates EC proliferation, 1886 cell cycle-related genes based on GO annotation were selected for further analyses (Suppl. Fig. 7D and Suppl. Table 1). Among those genes, CDKN1A/p21

Fig. 4 ALK2 regulates the proliferation of venous endothelial cells in the oxygen-induced retinopathy model. **A** Schematic diagram of the experimental design for the oxygen-induced retinopathy (OIR) model. Postnatal pups and their nursing female were exposed to 75% oxygen from P7 to P12 and returned to room air at P12 until further analysis. Tamoxifen (TM) was intraperitoneally injected at P11 and P12 to delete *Alk2* in ECs. **B** P17 retinal vasculature of OIR model. White dots depict the newly formed branch points. (Colors: IB4 (red) and EdU (green); Symbols: arteries (white arrowheads), veins (green arrowheads); Scale bar=250 μ M). **C–D** Quantification of the number of sprouts (**C**; $n=3$ (30 vessels from 6 retinas), $***P<0.0005$ (unpaired *t*-test)) and EdU⁺ ECs (**D**; $n=3$ (30 vessels from 6 retinas), $***P<0.0005$ (unpaired *t*-test)) shown in panel B. **E** ALK2 is highly expressed in the venous vascular tufts in the retinal vasculature of the OIR model. (Colors: IB4 (red) and ALK2 (green); Symbols: arteries (white arrowheads), veins (green arrowheads); Scale bar=100 μ M). **F** P14 retinal vasculature of WT (left panels) or *Alk2*^{ieCKO} OIR model (right panels). The area within the white dashed line is where vascular tufts were formed. The area within the white rectangles is at a higher magnification in the two bottom panels. (Colors: IB4 (red) and EdU (green); Scale bar=250 μ M). **G–H** Quantification of vascular tuft size (**G**; $n=3$ (34 vessels from 6 retinas), $***P<0.0005$ (unpaired *t*-test)) and the EdU⁺ ECs in tuft areas (**H**; $n=3$ (34 vessels from 6 retinas), $***P<0.0005$ (unpaired *t*-test)) shown in panel F. **I** P17 retinal vasculature in WT (top panels) or *Alk2*^{ieCKO} (bottom panels) mice of the OIR model. White dots indicate the newly formed branch points. (Colors: IB4 (red) and EdU (green); Scale bar=300 μ M). **J–K** Quantification of the number of sprouts (**J**; $n=3$ (36 vessels from 6 retinas), $***P<0.0005$ (unpaired *t*-test)) and EdU⁺ ECs (**K**; $n=3$ (36 vessels from 6 retinas), $***P<0.0005$ (unpaired *t*-test)) shown in panel H. **L** P17 retinal vasculature in WT (top panels) or *Alk2*^{ieCKO} (bottom panels) mice of the OIR model, stained for IB4 (white) (Scale bar=50 μ M). Inset images on the top right corner show avascular regions within the retina (red). Lack of ALK2 attenuates the neo-formation of vascular tufts in the OIR model. **M** Quantification of the avascular region ($n=3$ (32 vessels from 6 retinas), $***P<0.0005$ (unpaired *t*-test)) shown in panel L

(p21 hereafter), a negative modulator of cell cycle progression [4], was significantly upregulated (Fig. 5A, and Suppl. Fig. 7E). Consistent with this finding, quantitative RT-PCR and western blot (Fig. 5B–D) showed that p21 was upregulated in *ALK2* siRNA-treated HUVECs compared to controls. Moreover, immunostaining for p21 and EdU labeling showed that p21 expression was elevated in the absence of ALK2, with a concomitant decrease of EdU⁺ ECs (Fig. 5E, F, and Suppl. Fig. 7F). Similarly, the lack of endothelial ALK2 significantly increased the expression of p21 and reduced the number of EdU⁺ cells in the murine retinal veins (Fig. 5G, H, and Suppl. Fig. 8A). In addition, reducing p21 expression in *ALK2* siRNA-treated HUVECs partially restored the number of EdU⁺ cells (Suppl. Fig. 9A–F). Conversely, ectopic expression of p21 decreased the number of EdU⁺ cells both in cell culture and murine retinal vessels (Suppl. Fig. 9G–J). Taken together, our data reiterate the importance of p21 as a downstream target for ALK2 in modulating EC proliferation. Interestingly, the lack of ALK2 did not alter the expression of p53, a well-characterized upstream activator of p21 or p27, which has been previously implicated in regulating endothelial proliferation (Suppl.

Fig. 10A–D), suggesting that ALK2 selectively regulates p21 expression by a yet unidentified mechanism. The effects of ALK2 on p21 expression appear to be unique since inhibition of ALK1 or BMPR2 did not induce any discernible increase in p21 expression (Suppl. Fig. 10E).

Considering that ALK2 functions as a surface receptor and transduces signals through mediators such as SMAD1/5 and ERK1/2 [35], we hypothesized that it might regulate the expression of p21 via these downstream effectors. In HUVECs treated with *SMAD1/5* siRNA, both p21 transcript and protein were substantially increased (Fig. 5I, J), corroborating the effects of *ALK2* siRNA on p21. In addition, attenuation of *SMAD4* similarly elevated the expression of p21 (Suppl. Fig. 11A–C). Therefore, SMAD1/5 may mediate the ALK2-dependent regulation of p21 expression. Interestingly, chromatin immunoprecipitation did not reveal direct binding of SMAD1/5 to the p21 promoter, suggesting an indirect transcriptional regulation mechanism (Suppl. Fig. 11D–G). Taken together, our data illustrate that ALK2 is essential to restrict the expression of p21 and, therefore, permits the progression of the cell cycle in ECs (Fig. 5K).

Discussion

Previously, we and others reported that BMP signaling could provide a context-dependent pro-angiogenic function [16–20, 36–38]. However, the molecular mechanisms, including corresponding receptors and downstream signaling cascades, are largely unknown. This study demonstrates that ALK2 promotes cell cycle progression and subsequent proliferation in ECs during developmental and pathological angiogenesis. Consistently, endothelial deletion of ALK2 in mice led to severe vascular defects, which were more pronounced in venous vascular beds. Mechanistically, ALK2 modulates the expression of p21, a key negative regulator of cell cycle progression and a critical factor for balancing proliferation and migration in ECs. Based on our data, we propose that BMP signaling modulates the behavior of ECs via ALK2 activity.

We find that venous ECs are more proliferative than arterial ECs. While the underlying mechanisms that create the differences in proliferative capacity between arterial and venous ECs remain elusive, it is apparent that ALK2 appears to be required to modulate endothelial proliferation. Our data suggest that ALK2 restricts the level of p21 expression, thereby allowing endothelium to respond more robustly to angiogenic stimuli supplied by BMP ligands (Fig. 5K). As p21 is a key negative modulator for cell cycle progression, as well as migratory behaviors during angiogenesis [39], fine-tuning of p21 expression is essential to balance proliferation and migration of ECs during angiogenesis. Moreover, fine-tuning of p21

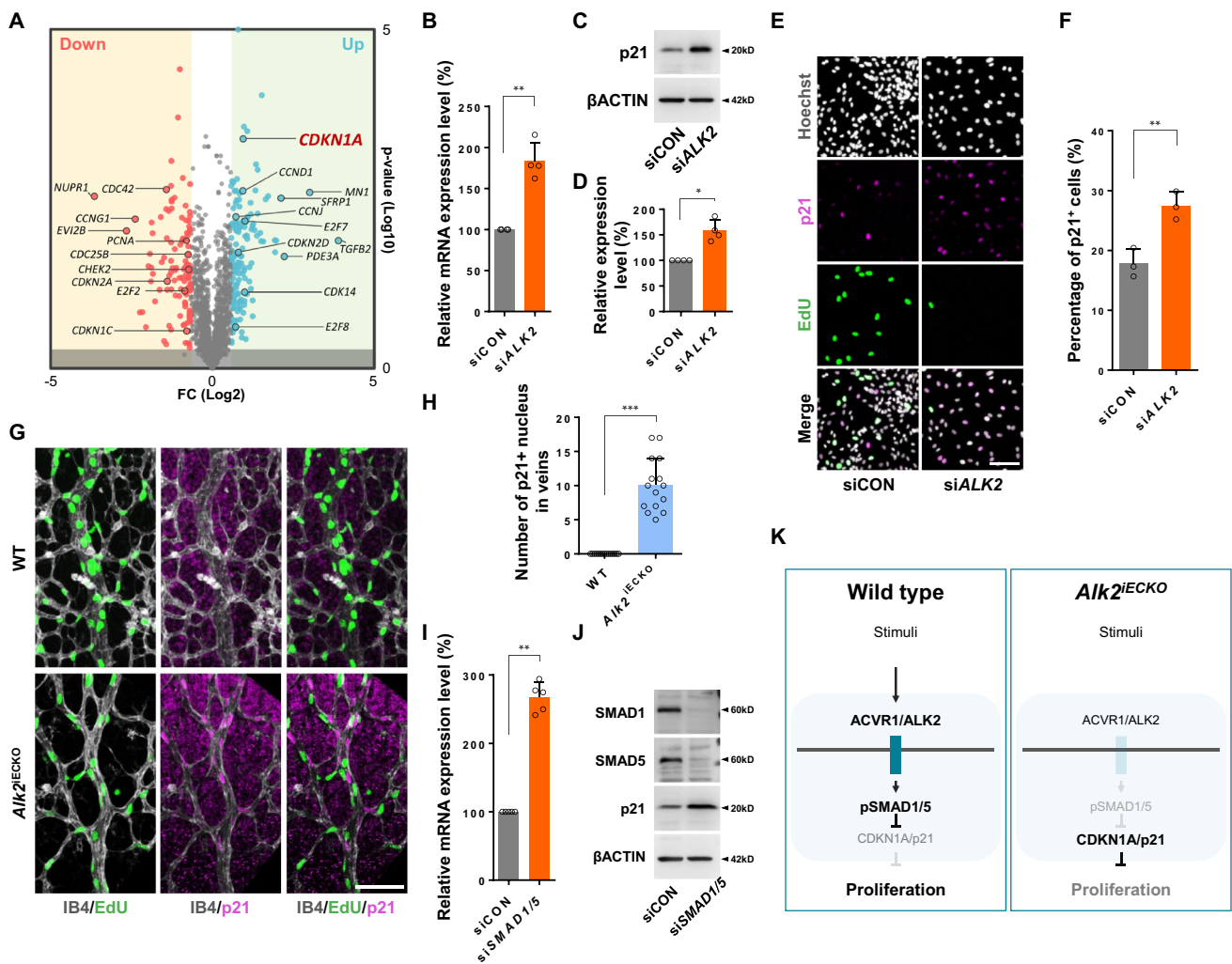


Fig. 5 ALK2-SMAD-p21 axis regulates endothelial proliferation. **A** Volcano plot showing genes of which expression was altered by the absence of *ALK2* in HUVEC. The positions of upregulated and downregulated transcripts were labeled in the plot along with key cell cycle-related transcripts. *CDKN1A/p21* is one of the significantly upregulated transcripts in *ALK2* siRNA-treated HUVECs. **B** Relative expression level of *CDKN1A/p21* mRNA in *ALK2* siRNA-treated HUVECs compared to control. ($n=4$, $**P < 0.005$ (unpaired *t*-test)). **C–D** *CDKN1A/p21* protein expression is elevated in *ALK2* siRNA-treated HUVECs. (**C**). Quantification of *CDKN1A/p21* protein expression (**D**; $n=4$, $*P < 0.05$ (unpaired *t*-test)) is shown as well. **E–F** Depletion of *ALK2* increases *CDKN1A/p21* expression and attenuates cell proliferation in HUVECs. (**E**; Colors: Hoechst (white), p21 (magenta), and EdU (green); Scale bar = 100 μ m) Quantification

of p21⁺ ECs in percentage is shown. (**F**; $n=3$, $**P < 0.005$ (unpaired *t*-test)). **G** Depletion of *ALK2* increases the number of p21-expressing venous ECs in the retinal vasculature. (Colors: IB4 (grey), EdU (green), and p21 (magenta); Scale bar = 100 μ m). **H** Quantification of the number of p21⁺ venous ECs shown in panel G. ($n=3$ (28 veins from 6 retinas), $***P < 0.0005$ (unpaired *t*-test)). **I** Inhibition of *SMAD1/5* expression shows an elevated level of *CDKN1A/p21* transcript in HUVECs. ($n=5$, $**P < 0.005$ (unpaired *t*-test)). **J** Depletion of *SMAD1/5* increases *CDKN1A/p21* protein levels in HUVECs. **K** Working model: The preferential enrichment of *ALK2* protein in venous ECs suggests its role in priming these cells for proliferation by restricting p21 expression in a *SMAD1/5*-dependent manner. Therefore, the presence of *ALK2* protein facilitates cell cycle progression and promotes proliferation, specifically in venous ECs

expression in the endothelium, in particular, in venous ECs, is likely more important as they are the primary source of newly formed ECs during angiogenesis [27]. It is noteworthy that we did not find any discernible number of proliferating ECs in the arterial vascular beds. Moreover, we were not able to observe any substantial increase in

p21 expression within arterial vascular beds in the retina upon *Alk2* deletion. Since the Cre driver appears to be active in both arterial and venous ECs, combined with previous reports that the Notch-p27 axis is important in modulating proliferation of ECs [40], our observations

allude an intriguing possibility that proliferation of ECs may be regulated by an array of regulators in a subtype-dependent manner.

Our data show that the lack of ALK2 elevates the expression of p21. Interestingly, inhibition of other BMPR1s or BMPR2 did not elicit similar effects on p21 expression, indicating that ALK2 has a unique function in modulating the cell cycle in response to BMP signaling. In addition, activation of ALK2 did not elicit any apparent effects on p21 expression, which contradicts previous reports that activation of TGF β signaling increases p21 expression and thereby promotes cell cycle arrest in tumor cells [41]. It is possible that the differences in cell type may create this discrepancy. Alternatively, it may reflect fundamental differences between TGF β and BMP signaling. Further analyses are warranted to delineate the precise molecular mechanisms underlying ALK2-mediated regulation of p21 expression and comparison between TGF β and BMP signaling on p21 expression. How does ALK2 modulate p21 expression? While the presence or absence of ALK2 protein apparently affects the level of p21 expression, p53, known to induce transcription of p21, did not change upon ALK2 manipulation. In addition, while we find that ALK2 regulation of p21 expression depends on SMAD1/5, it appears that SMAD1/5 does not directly bind to the p21 promoter. Therefore, it appears that ALK2 regulates p21 indirectly, perhaps via SMAD1/5 downstream targets, such as ID family members, that are transcriptional regulators [7].

Overall, our data show that ALK2 is required for venous EC proliferation during both developmental and pathological angiogenesis. We show that ALK2 protein is enriched in veins, which increases sensitivity toward BMP stimulation. Currently available anti-angiogenic strategies predominantly target VEGF signaling with a varying degree of success, often associated with unexpected complications. However, with recent findings that venous ECs continue to proliferate and serve as the primary source for newly formed ECs during angiogenesis, developing more selective treatment options by targeting proliferating venous ECs could increase the efficacy of anti-angiogenic treatments. While additional studies are warranted to fully comprehend the role of ALK2 in modulating endothelial proliferation in pathological settings, our finding that ALK2 is a key regulator of venous proliferation and functions as a potential nexus for integrating BMP and cell cycle progression presents an intriguing possibility that targeting ALK2 could serve as a promising yet previously unexploited target of anti-angiogenic therapies.

Supplementary Information The online version contains supplementary material available at <https://doi.org/10.1007/s10456-024-09936-6>.

Acknowledgements We thank Drs. Ralf Adams and Vesa Kaartinen for providing mice strains.

Author contributions B.P., M.K., O.H., H.-W.L., A.D., W.C., K.B., H.C., and K.M.C. performed the experiments, J.M.Y. and I.K. provided key reagents and technical advice, A.E., V.L.B., and S.-W.J. supervised the experiments. B.P., O.H., and S.-W.J. wrote the manuscript. All authors reviewed the manuscript.

Funding This work was supported by grants from National Institute of Health (HL114820 to SWJ), and grants from National Research Foundation of Korea (2019R1A2C2088125 and RS-2023-00208270 to SWJ, and 2022R1A6A3A13069135 to BP).

Declarations

Competing interests None.

References

- Kulikauskas MR, Shaka X, Bautch VL (2022) The versatility and paradox of BMP signaling in endothelial cell behaviors and blood vessel function. *Cell Mol Life Sci* 79(2):77. <https://doi.org/10.1007/s00018-021-04033-z>
- Luo W, Garcia-Gonzalez I, Fernandez-Chacon M, Casquero-Garcia V, Sanchez-Munoz MS, Muhleder S, Garcia-Ortega L, Andrade J, Potente M, Benedito R (2020) Arterialization requires the timely suppression of cell growth. *Nature*. <https://doi.org/10.1038/s41586-020-3018-x>
- Weijts B, Gutierrez E, Saikin SK, Ablooglu AJ, Traver D, Grosman A, Tkachenko E (2018) Blood flow-induced Notch activation and endothelial migration enable vascular remodeling in zebrafish embryos. *Nat Commun* 9:5314. <https://doi.org/10.1038/s41467-018-07732-7>
- Fang JS, Coon BG, Gillis N, Chen ZH, Qiu JY, Chittenden TW, Burt JM, Schwartz MA, Hirschi KK (2017) Shear-induced Notch-Cx37-p27 axis arrests endothelial cell cycle to enable arterial specification. *Nat Commun* 8. <https://doi.org/10.1038/s41467-017-01742-7>
- Luo W, Garcia-Gonzalez I, Fernandez-Chacon M, Casquero-Garcia V, Sanchez-Munoz MS, Muhleder S, Garcia-Ortega L, Andrade J, Potente M, Benedito R (2021) Arterialization requires the timely suppression of cell growth. *Nature* 589(7842):437–441. <https://doi.org/10.1038/s41586-020-3018-x>
- Kim JD, Lee HW, Jin SW (2014) Diversity is in my veins: role of bone morphogenetic protein signaling during venous morphogenesis in zebrafish illustrates the heterogeneity within endothelial cells. *Arterioscler Thromb Vasc Biol* 34(9):1838–1845. <https://doi.org/10.1161/ATVBAHA.114.303219>
- Langenfeld EM, Langenfeld J (2004) Bone morphogenetic protein-2 stimulates angiogenesis in developing tumors. *Mol Cancer Res* 2(3):141–149
- Valdimarsdottir G, Goumans MJ, Rosendahl A, Brugman M, Itoh S, Lebrin F, Sideras P, ten Dijke P (2002) Stimulation of Id1 expression by bone morphogenetic protein is sufficient and necessary for bone morphogenetic protein-induced activation of endothelial cells. *Circulation* 106(17):2263–2270
- Cuttano R, Rudini N, Bravi L, Corada M, Giampietro C, Papa E, Morini MF, Maddaluno L, Baeyens N, Adams RH, Jain MK, Owens GK, Schwartz M, Lampugnani MG, Dejana E (2016) KLF4 is a key determinant in the development and progression of cerebral cavernous malformations. *EMBO Mol Med* 8(1):6–24. <https://doi.org/10.15252/emmm.201505433>

10. Tillet E, Bailly S (2014) Emerging roles of BMP9 and BMP10 in hereditary hemorrhagic telangiectasia. *Front Genet* 5:456. <https://doi.org/10.3389/fgene.2014.00456>
11. Ola R, Kunzel SH, Zhang F, Genet G, Chakraborty R, Pibouin-Fragner L, Martin K, Sessa W, Dubrac A, Eichmann A (2018) SMAD4 prevents flow induced arteriovenous malformations by inhibiting casein kinase 2. *Circulation* 138(21):2379–2394. <https://doi.org/10.1161/CIRCULATIONAHA.118.033842>
12. Aspalter IM, Gordon E, Dubrac A, Ragab A, Narloch J, Vizan P, Geudens I, Collins RT, Franco CA, Abrahams CL, Thurston G, Fruttiger M, Rosewell I, Eichmann A, Gerhardt H (2015) Alk1 and Alk5 inhibition by Nr1 controls vascular sprouting downstream of Notch. *Nat Commun* 6:7264. <https://doi.org/10.1038/ncomms8264>
13. Lee HW, Chong DC, Ola R, Dunworth WP, Meadows S, Ka J, Kaartinen VM, Qyang YB, Cleaver O, Bautch VL, Eichmann A, Jin SW (2017) Alk2/ACVR1 and Alk3/BMPRI1 provide essential function for bone morphogenetic protein-induced retinal angiogenesis. *Arterioscler Thromb Vasc Biol* 37(4):657–663. <https://doi.org/10.1161/atvbaha.116.308422>
14. Neal A, Nornes S, Payne S, Wallace MD, Fritzsche M, Louphrasitthiphol P, Wilkinson RN, Chouliaras KM, Liu K, Plant K, Sholapurkar R, Ratnayaka I, Herzog W, Bond G, Chico T, Bou-Gharios G, De Val S (2019) Venous identity requires BMP signalling through ALK3. *Nat Commun* 10(1):453. <https://doi.org/10.1038/s41467-019-08315-w>
15. Larrivee B, Prahst C, Gordon E, del Toro R, Mathivet T, Duarte A, Simons M, Eichmann A (2012) ALK1 signaling inhibits angiogenesis by cooperating with the Notch pathway. *Dev Cell* 22(3):489–500. <https://doi.org/10.1016/j.devcel.2012.02.005>
16. Benn A, Alonso F, Mangelschots J, Genot E, Lox M, Zwijsen A (2020) BMP-SMAD1/5 signaling regulates retinal vascular development. *Biomolecules* 10(3):488. <https://doi.org/10.3390/biom10030488>
17. Guihard PJ, Guo Y, Wu X, Zhang L, Yao J, Jumabay M, Yao Y, Garfinkel A, Bostrom KI (2020) Shaping waves of bone morphogenetic protein inhibition during vascular growth. *Circ Res* 127(10):1288–1305. <https://doi.org/10.1161/CIRCRESAHA.120.317439>
18. Tischfield MA, Robson CD, Gillette NM, Chim SM, Sofela FA, DeLisle MM, Gelber A, Barry BJ, MacKinnon S, Dagi LR, Nathans J, Engle EC (2017) Cerebral vein malformations result from loss of twist1 expression and BMP signaling from skull progenitor cells and dura. *Dev Cell* 42(5):445–461.e5. <https://doi.org/10.1016/j.devcel.2017.07.027>
19. Wakayama Y, Fukuhara S, Ando K, Matsuda M, Mochizuki N (2015) Cdc42 mediates Bmp-induced sprouting angiogenesis through Fmn13-driven assembly of endothelial filopodia in zebrafish. *Dev Cell* 32(1):109–122. <https://doi.org/10.1016/j.devcel.2014.11.024>
20. Wiley DM, Kim JD, Hao JJ, Hong CC, Bautch VL, Jin SW (2011) Distinct signalling pathways regulate sprouting angiogenesis from the dorsal aorta and the axial vein. *Nat Cell Biol* 13(6):686–692. <https://doi.org/10.1038/ncb2232>
21. Eisa-Beygi S, Hu MM, Kumar SN, Jeffery BE, Collery RF, Vo NJ, Lamichanne BS, Yost HJ, Veldman MB, Link BA (2023) Mesenchymal stromal cells facilitate tip cell fusion downstream of BMP-mediated venous angiogenesis-brief report. *Arterioscler Thromb Vasc Biol* 43(7):e231–e237. <https://doi.org/10.1161/ATVBAHA.122.318622>
22. Upton PD, Park JES, De Souza PM, Davies RJ, Griffiths MJD, Wort SJ, Morrell NW (2020) Endothelial protective factors BMP9 and BMP10 inhibit CCL2 release by human vascular endothelial cells. *J Cell Sci* 133(14). <https://doi.org/10.1242/jcs.239715>
23. Li W, Salmon RM, Jiang H, Morrell NW (2016) Regulation of the ALK1 ligands, BMP9 and BMP10. *Biochem Soc Trans* 44(4):1135–1141. <https://doi.org/10.1042/BST20160083>
24. Friedrichs M, Wirsdoerfer F, Flohe SB, Schneider S, Wuelling M, Vortkamp A (2011) BMP signaling balances proliferation and differentiation of muscle satellite cell descendants. *BMC Cell Biol* 12:26. <https://doi.org/10.1186/1471-2121-12-26>
25. Bhardwaj G, Murdoch B, Wu D, Baker DP, Williams KP, Chadwick K, Ling LE, Karanu FN, Bhatia M (2001) Sonic hedgehog induces the proliferation of primitive human hematopoietic cells via BMP regulation. *Nat Immunol* 2(2):172–180. <https://doi.org/10.1038/84282>
26. Suzuki Y, Ohga N, Morishita Y, Hida K, Miyazono K, Watabe T (2010) BMP-9 induces proliferation of multiple types of endothelial cells in vitro and in vivo. *J Cell Sci* 123(Pt 10):1684–1692. <https://doi.org/10.1242/jcs.061556>
27. Lee HW, Xu Y, He L, Choi W, Gonzalez D, Jin SW, Simons M (2021) Role of venous endothelial cells in developmental and pathologic angiogenesis. *Circulation* 144(16):1308–1322. <https://doi.org/10.1161/CIRCULATIONAHA.121.054071>
28. Kaartinen V, Nagy A (2001) Removal of the floxed neo gene from a conditional knockout allele by the adenoviral Cre recombinase in vivo. *Genesis* 31(3):126–129. <https://doi.org/10.1002/gene.10015>
29. Benedito R, Roca C, Sorensen I, Adams S, Gossler A, Fruttiger M, Adams RH (2009) The notch ligands Dll4 and Jagged1 have opposing effects on angiogenesis. *Cell* 137(6):1124–1135. <https://doi.org/10.1016/j.cell.2009.03.025>
30. Pitulescu ME, Schmidt I, Giaimo BD, Antoine T, Berkenfeld F, Ferrante F, Park H, Ehling M, Biljes D, Rocha SF, Langen UH, Stehling M, Nagasawa T, Ferrara N, Borggreffe T, Adams RH (2017) Dll4 and Notch signalling couples sprouting angiogenesis and artery formation. *Nat Cell Biol* 19(8):915–927. <https://doi.org/10.1038/ncb3555>
31. Weckbach LT, Preissner KT, Deindl E (2018) The role of midkine in arteriogenesis, involving mechanosensing, endothelial cell proliferation, and vasodilation. *Int J Mol Sci* 19(9):2559. <https://doi.org/10.3390/ijms19092559>
32. Mohedas AH, Wang Y, Sanvitale CE, Canning P, Choi S, Xing X, Bullock AN, Cuny GD, Yu PB (2014) Structure-activity relationship of 3,5-diaryl-2-aminopyridine ALK2 inhibitors reveals unaltered binding affinity for fibrodysplasia ossificans progressiva causing mutants. *J Med Chem* 57(19):7900–7915. <https://doi.org/10.1021/jm501177w>
33. Carvalho D, Taylor KR, Olaciregui NG, Molinari V, Clarke M, Mackay A, Ruddle R, Henley A, Valenti M, Hayes A, Brandon AH, Eccles SA, Raynaud F, Boudhar A, Monje M, Popov S, Moore AS, Mora J, Cruz O, Vinci M, Brennan PE, Bullock AN, Carcaboso AM, Jones C (2019) ALK2 inhibitors display beneficial effects in preclinical models of ACVR1 mutant diffuse intrinsic pontine glioma. *Commun Biol* 2:156. <https://doi.org/10.1038/s42003-019-0420-8>
34. Vahatupa M, Jarvinen TAH, Uusitalo-Jarvinen H (2020) Exploration of oxygen-induced retinopathy model to discover new therapeutic drug targets in retinopathies. *Front Pharmacol* 11:873. <https://doi.org/10.3389/fphar.2020.00873>
35. Atri D, Larrivee B, Eichmann A, Simons M (2013) Endothelial signaling and the molecular basis of arteriovenous malformation. *Cell Mol Life Sci*. <https://doi.org/10.1007/s00018-013-1475-1>
36. Mouillesseaux KP, Wiley DS, Saunders LM, Wylie LA, Kushner EJ, Chong DC, Citrin KM, Barber AT, Park Y, Kim JD, Samsa LA, Kim J, Liu J, Jin SW, Bautch VL (2016) Notch regulates BMP responsiveness and lateral branching in vessel networks via

- SMAD6. *Nat Commun* 7:13247. <https://doi.org/10.1038/ncomms13247>
37. Benn A, Hiepen C, Osterland M, Schutte C, Zwijsen A, Knaus P (2017) Role of bone morphogenetic proteins in sprouting angiogenesis: differential BMP receptor-dependent signaling pathways balance stalk vs. tip cell competence. *FASEB J* 31(11):4720–4733. <https://doi.org/10.1096/fj.201700193RR>
38. Ren R, Charles PC, Zhang C, Wu Y, Wang H, Patterson C (2007) Gene expression profiles identify a role for cyclooxygenase 2-dependent prostanoid generation in BMP6-induced angiogenic responses. *Blood* 109(7):2847–2853. <https://doi.org/10.1182/blood-2006-08-039743>
39. Kiosses WB, Daniels RH, Otey C, Bokoch GM, Schwartz MA (1999) A role for p21-activated kinase in endothelial cell migration. *J Cell Biol* 147(4):831–844. <https://doi.org/10.1083/jcb.147.4.831>
40. Fang JS, Coon BG, Gillis N, Chen Z, Qiu J, Chittenden TW, Burt JM, Schwartz MA, Hirschi KK (2017) Shear-induced Notch-Cx37-p27 axis arrests endothelial cell cycle to enable arterial specification. *Nat Commun* 8(1):2149. <https://doi.org/10.1038/s41467-017-01742-7>
41. Zhang Y, Alexander PB, Wang XF (2017) TGF-beta family signaling in the control of cell proliferation and survival. *Cold Spring Harb Perspect Biol* 9(4). <https://doi.org/10.1101/cshperspect.a022145>

Publisher's Note Springer Nature remains neutral with regard to jurisdictional claims in published maps and institutional affiliations.

Springer Nature or its licensor (e.g. a society or other partner) holds exclusive rights to this article under a publishing agreement with the author(s) or other rightsholder(s); author self-archiving of the accepted manuscript version of this article is solely governed by the terms of such publishing agreement and applicable law.